Ocean Dynamics (2014) 64:1657–1670
DOI 10.1007/s10236-014-0774-x

Unified global and regional wave model on a multi-resolution grid

Jian-Guo Li · Andrew Saulter

Received: 21 January 2014 / Accepted: 17 September 2014 / Published online: 2 October 2014

Abstract Models for ocean surface wave forecasting in weather centres comprise global and regional systems in order to efficiently meet service demands. Regional models cannot run alone and have to use large area or global models to provide boundary wave spectra. The modern two-way nesting technique is to run the two models together with the regional model domain covered by both resolutions. An alternative method is to use a single multi-resolution grid that fits irregular coastlines and provides refined resolutions in selected regions. This paper presents a multi-resolution model based on a spherical multiple-cell (SMC) grid, which is designed to relax the CFL restriction of Eulerian advection time step at high latitudes by merging the conventional latitude-longitude grid cells. The implementation of the SMC grid in WAVEWATCH III is described, and a multi-resolution (6, 12 and 25 km) global SMC configuration is compared with a suite of nested grid ocean surface wave models, including 35-km global, 8-km European and 4-km UK regional models. Verification against buoy and platform wave observations indicates that the unified model is better than the 35-km global and very close in performance to the two regional models.

Keywords Multi-resolution · Unstructured grid · Ocean surface wave · Nested model · Polar problem

Responsible Editor: Oyvind Breivik

This article is part of the Topical Collection on the *13th International Workshop on Wave Hindcasting and Forecasting in Banff, Alberta, Canada October 27 - November 1, 2013*

J.-G. Li (✉) · A. Saulter
Met Office, FitzRoy Road, Exeter EX1 3PB, United Kingdom
e-mail: Jian-Guo.Li@metoffice.gov.uk

1 Introduction

Models for ocean surface wave forecasting in weather centres comprise global and regional systems in order to efficiently meet service demands. Most regional models aim to resolve details near coastlines and be compatible with high resolution atmospheric models. However, these regional models cannot run alone and have to use large area or global models to provide boundary wave spectra. The most traditional nesting technique is to run the two models together with the regional model domain covered by both resolutions. Two-way nesting schemes have also been developed, but still require an overlapping 'stencil area' (Tolman 2008). Using an unstructured grid technique, this nested model system may be replaced with a multi-resolution model so both the domain overlapping and boundary condition for the regional model may be avoided. A review of grid schemes that can be used to construct such models is given in Li (2012).

A spherical multiple-cell (SMC) grid (Li 2011) has been developed and implemented in the WAVEWATCH III ocean surface wave model (Tolman 1991; Tolman et al. 2002). The SMC grid is designed to relax the CFL restriction of Eulerian advection time step at high latitudes by merging the conventional latitude-longitude grid cells as in the reduced grid (Rasch 1994). High resolution is achieved by mesh refinement, similar to the quadtree-adaptive grid in the WAVEWATCH III model (Popinet et al. 2010) but does not need to keep all the four refined cells within one coarse cell as the quadtree grid does. In order to accomplish these flexibilities, the SMC grid follows a method common to 'unstructured' grids where cells are not arranged in a rectangular array form, but are instead listed as a 1-D array and linked via cell and face identifiers, similar to the triangle cell unstructured grid in the WAVEWATCH III model (Roland et al. 2009). Li

(2012) describes the application of the SMC grid in wave models and how to solve the polar problems by fixing the wave spectral reference direction within a high latitude circle. It allows wave models to be extended to high latitudes or even the whole Arctic if the Arctic sea ice disappears in future summers. Furthermore, the unstructured features of the SMC grid allows land cells to be removed from the model, boundaries to fit irregular coastlines and the support of refined resolutions with reduced sub-time steps. This latter feature, and the fact that the SMC grid retains finite-difference schemes on a conventional latitude-longitude mesh, leads to an efficient multi-resolution grid. Additional efficiencies have been incorporated into wave propagation schemes, including an upstream non-oscillatory second-order (UNO2) advection scheme (Li 2008), which saves about 30 % advection time in comparison with the original third-order scheme, and a rotational refraction scheme, which removes the refraction angle limit imposed by the original advection alike refraction scheme.

Unresolved small island groups in global coarse resolution wave models lead to a persistent over-estimation of ocean swell energy as island blocking is an important sink of the wave energy (Tolman 2003). This swell over-estimation is alleviated, particularly in the far field, with the introduction of sub-grid obstructions; however, high resolution around islands is still the most appropriate approach for accurate swell prediction close to islands (Chawla and Tolman 2008). The SMC grid can resolve small islands and coastlines with refined resolutions while keeping the vast open oceans at an affordable resolution. While refined resolution at operational global model scales does not completely alleviate the need to use sub-grid obstruction, improved representation of islands (particularly those with complex shape) is an additional advantage of this unified model.

The features of the SMC grid make it an ideal candidate scheme for application in global or large area models typically run by National Meteorological Services, as a replacement or alternative to a multi-model suite. This paper outlines the essential formulation of the SMC grid and illustrates its application to continental shelf seas wave forecasting, based on a unified model configuration at 25-km global resolution and refined 12- and 6-km resolutions near coastlines and in the European region. The three-tiered (6-12-25 km) global multi-resolution SMC grid (SMC6125) has previously been validated with satellite and buoy data and compared with a 25-km global latitude-longitude model (Li 2012; Li and Saulter 2012). Here, the SMC6125 grid is compared with outputs from a traditional nested model suite, comprising the Met Office operational global 35-km (G35) grid and European 8-km (EU8) and UK 4-km (UK4) regional grids.

2 The SMC grid WAVEWATCH III model

The WAVEWATCH III ocean surface wave model is a community model developed by a group of wave modellers, particularly Hendrik Tolman (Tolman 1991; Tolman et al. 2002, Tolman et al. 2013). Since 2008, the Met Office has joined the development group and contributed to the implementation of a second-order advection scheme, a rotated grid and the SMC grid in the WAVEWATCH III model, which is recently released at version 4.18 (Tolman HL and the WAVEWATCH III® development group 2014). The unified global and regional wave model is based on the WAVEWATCH III model using the SMC grid. The global propagation of ocean surface waves on the SMC grid is given by Li (2011, 2012), and here, we only outline the SMC grid-related changes in the WAVEWATCH III model.

2.1 Wave energy balance equation

Because the SMC grid is virtually a latitude-longitude grid, it uses the same Eulerian ocean surface wave 2-D spectral energy balance equation as on a spherical latitude-longitude grid. In the 2-D spherical coordinates with longitude λ and latitude φ, the equation is given by

$$\frac{\partial \psi}{\partial t}+\frac{\partial F_x}{\partial x}+\frac{\partial\left(F_y\cos\varphi\right)}{\cos\varphi\partial y}+\frac{\partial\left(\dot{k}\psi\right)}{\partial k}+\frac{\partial\left(\dot{\theta}\psi\right)}{\partial\theta}=S \qquad (1)$$
$$F_x \equiv u\psi - D_x\partial\psi/\partial x$$
$$F_y \equiv v\psi - D_y\partial\psi/\partial y$$

where $\psi(t, \lambda, \varphi, k, \theta)$ is any component of the wave energy spectrum, t is the time, k is the wave number, θ is the spectral direction (usually defined from the local east direction), u and v are the zonal and meridional components of the wave energy propagation speed, D_x and D_y are the diffusion coefficients and S is the source term. The geophysical coordinates x and y are defined locally eastward along the parallel and northward along the meridian, respectively. Their increments are given by $dx=r\cos\varphi d\lambda$, $dy=rd\varphi$, where r is the radius of the sphere. The overhead dot indicates time differentiation along the wave propagation path. The r.h.s S represents all source terms, and they are unchanged from the original WAVEWATCH III model. Note that in WAVEWATCH III model, the wave action $A\equiv\psi/\omega$, where ω is the intrinsic angular frequency of the ocean surface wave, is chosen instead of the wave energy ψ for conservation when ocean current is present. The wave action shares the same equation (Eq. 1) as the wave energy except that the source term is divided by ω. Hence, all propagation schemes for wave energy can be applied to wave action.

The spherical wave energy balance equation (Eq. 1) differs from its Cartesian counterpart in the meridian differential term by an extra cosine factor, which renders the term undefined

(singular) at the Poles. Thus, except for at the Poles, Eq. (1) can be approximated with finite-difference schemes similar to those used in the Cartesian grid. The only difference between the Cartesian and spherical versions of these finite-difference schemes is that the latter has an extra cosine factor. The diffusion term in Eq. (1) may be considered as the sub-grid mixing term because the model wave spectrum represents the spatial average over one grid cell. This diffusion term is usually parameterised to alleviate the so-called garden-sprinkler effect (GSE) due to discretisation of the wave energy spectrum (Booij and Holthuijsen 1987; Tolman 2002).

2.2 Advection-diffusion term

Because the SMC grid is an unstructured grid, its 1-D cell sequence is arbitrary in theory. For the multi-resolution SMC grid, its cells are listed in an order sorted by their sizes so that sub-time steps can be used conveniently for propagation over refined cells (Li 2012). Neighbouring cell information is stored in a face-array for each spatial dimension. The cell face with the normal velocity component u along the x-direction is called the u-face. Similarly, the cell face with the y-directional normal velocity component v is called the v-face. The advection flux with the UNO2 scheme and the diffusion flux with a central-space finite-difference scheme for a u-face between the central (C) and downstream (D) cells are merged into a single flux, given by

$$\Delta F_x = (u\psi * - D_x G_{DC}) l_u \Delta t \tag{2}$$

where ψ* is the mid-flux value evaluated with the UNO2 scheme (see Eq. (6) in Li 2008), $G_{DC}=(\psi_D-\psi_C)/(x_D-x_C)$ is the gradient between the central and downstream cells, l_u is the u-face length, and Δt is the sub-time step. The face length is included in the flux (Eq. 2) to count for the multi-resolution face sizes. Both the advection and diffusion schemes are of second-order accuracy. In the presence of an ambient ocean current, the wave energy propagation speed in the x-direction should be the sum of the x-components of the wave group speed, c_g, and the current speed, U, that is, $u=c_g\cos\theta+U_x$.

The diffusion coefficient, $D_x=D_y$, is chosen to be the transverse diffusion coefficient D_{nn} as defined in Booij and Holthuijsen (1987) and used in the WAVEWATCH III model. The transverse diffusion coefficient is determined by the spectral component propagation speed, directional bin width and a user input swell age parameter. The swell age has the same meaning as in the regular grid WAVEWATCH III model, and it has to be adjusted according to the base-level grid length and the advection-diffusion time step to ensure the maximum Fourier number is less than 1 (or usually set to be 0.5). A guide rule for the maximum swell age T_s is given by

$$D_x = \left(\frac{c_{\mathrm{gm}}\Delta\theta}{\Delta x_0}\right)^2 \frac{\Delta t_a T_s}{12} \le \frac{1}{2}, \quad or \quad T_s \le \frac{6}{\Delta t_a}\left(\frac{\Delta x_0}{c_{\mathrm{gm}}\Delta\theta}\right)^2 \tag{3}$$

in which Δt_a is the advection time step, Δx_0 is the base-level grid length on the Equator, $\Delta\theta$ is the directional bin width (in radian) and c_{gm} is the maximum deep water group speed in the model spectral range (usually at the lowest frequency end).

The l.h.s terms in Eq. (1) are calculated with time-splitting approaches by combining the first (time differential) term with each of the other four terms. The advection-diffusion terms are discretised on the SMC grid with one flux loop and one cell loop for each dimension. A temporary net-flux variable, F_{net}, is used for each cell to gather all fluxes into the cell before it is used for the cell value update. The use of face sizes and the net-flux variables allows fluxes from different sized faces to be added up in proportion to their sizes before each cell value is updated in a cell loop by

$$\psi^{n+1} = \psi^n + F_{\mathrm{net}}/(l_x l_y) \tag{4}$$

where $l_{x/y}$ is the cell x/y-length. The cell y-length is required for x-flux update to cancel the face length used in sum of the fluxes in proportion to the u-face length. The v-face fluxes are calculated similarly except for the additional latitude cosine factor.

An additional benefit of the SMC grid propagation scheme is the complete blocking by even a single-cell island. As two consecutive zero-boundary cells are added for each boundary cell face beyond the coastline in the SMC grid, any single-point island is virtually expanded into a five-point island in each dimension. As a result, wave energy cannot pass through such an ‘expanded island’ with any five-point advection scheme. Nevertheless, the sub-grid obstruction scheme from the original WAVEWATCH III model is kept to account for any unresolved islands by the refined resolutions. The sub-grid obstruction scheme follows the approach of Hardy et al. (2000) with some modifications by Tolman (2003).

2.3 Refraction and great circle turning

One primary physical process that affects surface wave propagation is depth-induced refraction. Refraction formulations in contemporary surface wave models are based on the linear wave theory, assuming slow-varying ocean depth (WISE group 2007). Refraction on the SMC grid follows the formulations in WAVEWATCH III (Tolman 1991):

$$\dot{k} = -\xi\,\mathbf{k}\cdot\nabla h - \mathbf{k}\cdot\nabla U_k \tag{5}$$

$$\dot{\theta}_{\mathrm{rfr}} = -\xi\,\mathbf{n}\cdot\nabla h - \mathbf{n}\cdot\nabla U_k \tag{6}$$

where $\mathbf{k}=(k\cos\theta, k\sin\theta)$ is the wave number vector, h is the water depth, ∇ is the 2-D gradient operator, U_k is the ambient

current velocity component along the **k**-direction, $\xi=\omega/\sinh(2kh)$ will be referred to as the *refraction factor* and $\mathbf{n}=(-\sin\theta, \cos\theta)$ is a unit vector normal to the **k**-direction to the left or at $\theta+\pi/2$. The wave number change rate (Eq. 5) is also known as the *spectral shift*, and the directional change rate (Eq. 6) is called the *refraction rate*. More details on derivation of these refraction rates are available in Li (2012).

Wave energy travels along the shortest route on the ocean surface, that is, along great circles on the sphere. So, a wave spectral component will not be confined at its defined direction but will shift gradually with latitude along its great circle path, a procedure known as *great circle turning* (GCT). Assuming the great circle direction is at an angle θ from the local east direction at latitude φ, the GCT rate along the propagation direction is then given by

$$\dot{\theta}_{\mathrm{gct}} = -\left(c_g/r\right)\cos\theta\tan\varphi \tag{7}$$

The net wave direction-changing rate used in Eq. (1) for the SMC grid is then the sum of the refraction rate (Eq. 6) and the GCT rate (Eq. 7).

In WAVEWATCH III, the refraction and GCT are calculated with an advection-like scheme, which is subject to the equivalent CFL limit, that is, the rotation increment should be less than one directional bin width (~10°) per time step. Here, for the SMC grid, a rotation scheme is substituted for the advection-like scheme to estimate the refraction and GCT term so that the CFL limit can be avoided. The rotation scheme is similar to a re-mapping advection scheme and is unconditionally stable. Although the rotation scheme does not have any limit on the refraction increment, the refraction angle should not pass beyond the depth gradient line (where $\mathbf{n}\cdot\nabla h=0$) as stated in the refraction rate (Eq. 6). This physical limiter on the total refraction angle is included in the rotation scheme. The angle between the spectral direction and the depth decrease direction is calculated by

$$\gamma = \cos^{-1}\left[-\left(h_x\cos\theta + h_y\sin\theta\right)/\sqrt{h_x^2+h_y^2}\right] \tag{8}$$

where h_x and h_y are the water depth gradient along x- and y-axis, respectively. Because the FORTRAN function ACOS returns a value between 0 and π, the maximum refraction angle (absolute value) is then chosen to be less than $\pi/2$ with $\Delta\theta_{\mathrm{mxrfr}}=\min(\eta,\ \gamma,\ \pi-\gamma)$. The constant η ($<\pi/2$) is a user-defined maximum refraction angle to reduce the refraction effect if required. If η is set to be less than one directional bin width, the rotation scheme will be equivalent to the original advection-like scheme in the WAVEWATCH III model without using sub-time steps. This simple rotation subroutine not only removes the time step restriction on the refraction angle but also adds an implicit diffusion in the θ direction. This additional smoothing in the transverse direction is desirable for wave models to mitigate the GSE.

The spectral shift term, fourth in Eq. (1), is calculated with an advection-like UNO2 scheme in the k-space because the spectral shift is usually small enough to meet the CFL condition. The term is calculated at the base time step for all cell spectra.

3 Comparison of SMC6125 model with a global-regional nested system

3.1 The SMC6125 model

In principle, a multi-resolution SMC grid can be defined using as many refinements as required by the user. In practical applications for operational forecasting purposes, computational resources and resolution of available wind forcing necessitate a pragmatic approach. In the case described here a three-tiered model based on a 25-km global cell size is evaluated. The global SMC6125 grid is shown in Fig. 1. For clarity, only the Arctic and European regions are shown here. The highest resolution of the SMC6125 grid (for size-1) cell is set to be $\Delta\lambda=360°/(1024*4)=0.3515625°/4$ and $\Delta\varphi=180°/(768*4)=0.234375°/4$, and the latitudinal grid length is about 6 km. The SMC grid uses only the sea points or cells and refines the resolution by two levels to 6 km around islands and coastlines, resulting in a global three-level (6-12-25 km) SMC grid on the ocean surface. Cells are merged longitudinally at high latitudes following the same rules in Li (2011) to relax the CFL restriction. A polar cell is introduced to avoid the singularity at the Pole, and a fixed reference direction is substituted for the local east within the red circle in Fig. 1 to maintain the scalar assumption for wave spectral components (Li 2012).

To approach the resolution of the Met Office European regional model (described in the next section), the SMC6125 grid is refined in the European region at 12-km resolution, which includes the UK waters, the Baltic Sea, the Black Sea and the Mediterranean Sea. Note that this refined region does not match exactly the European 8-km model domain as the latter uses a rotated grid. Because of the decrease of grid length with latitude, the SMC6125 refined 12-km resolution is very close to the rotated 8-km resolution in physical distance. The red 'Y' symbols in Fig. 1 indicate the buoy and platform sites, which are used for comparison with other models.

A significant wave height (SWH) field of the SMC6125 model as viewed from the same projection as Fig. 1 is shown in Fig. 2, and it confirms that the minimum sea ice edge around the beginning of September 2012 is still below 86° N, within the global part of the SMC6125 model. So, the

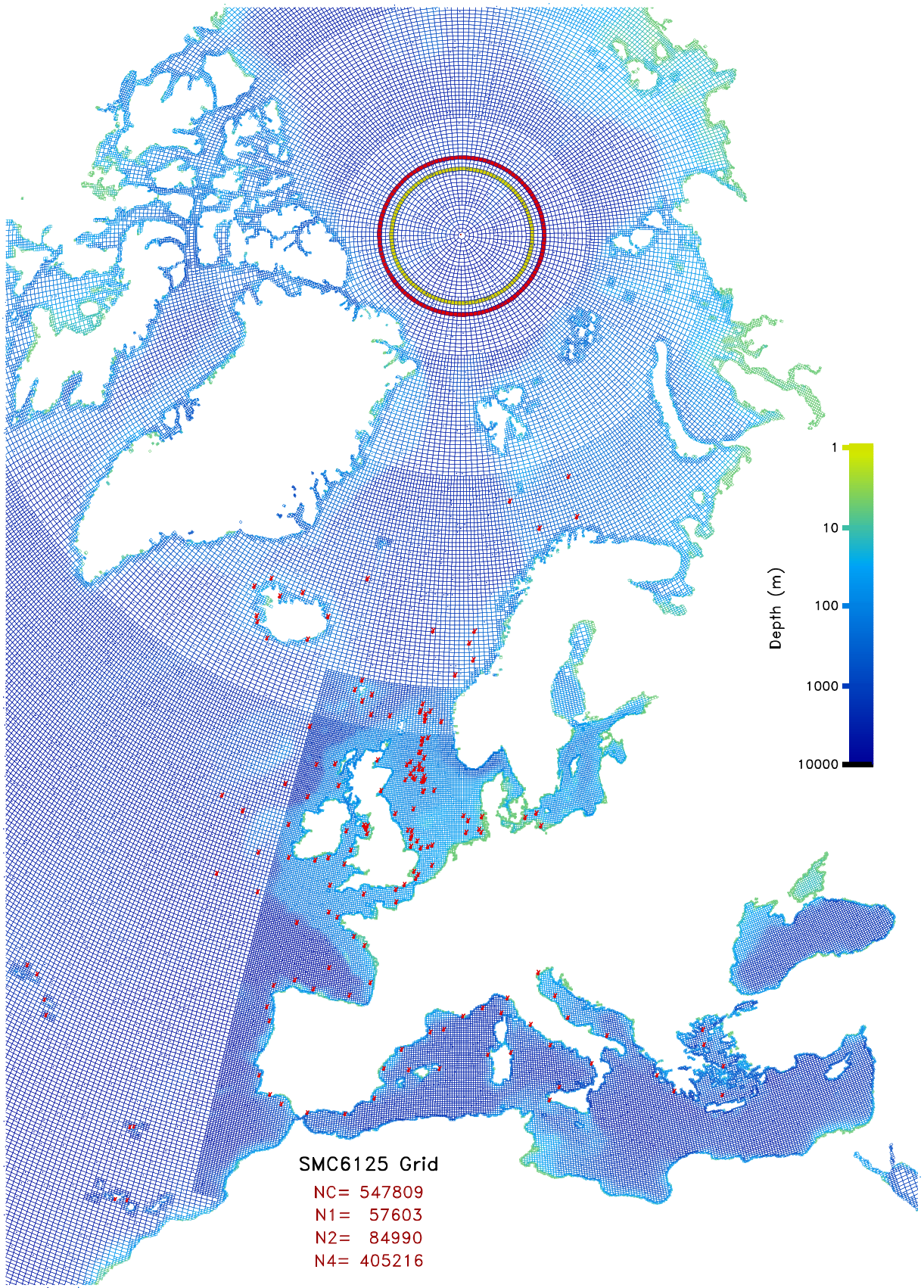

Fig. 1 The Arctic and European part of the SMC6125 grid

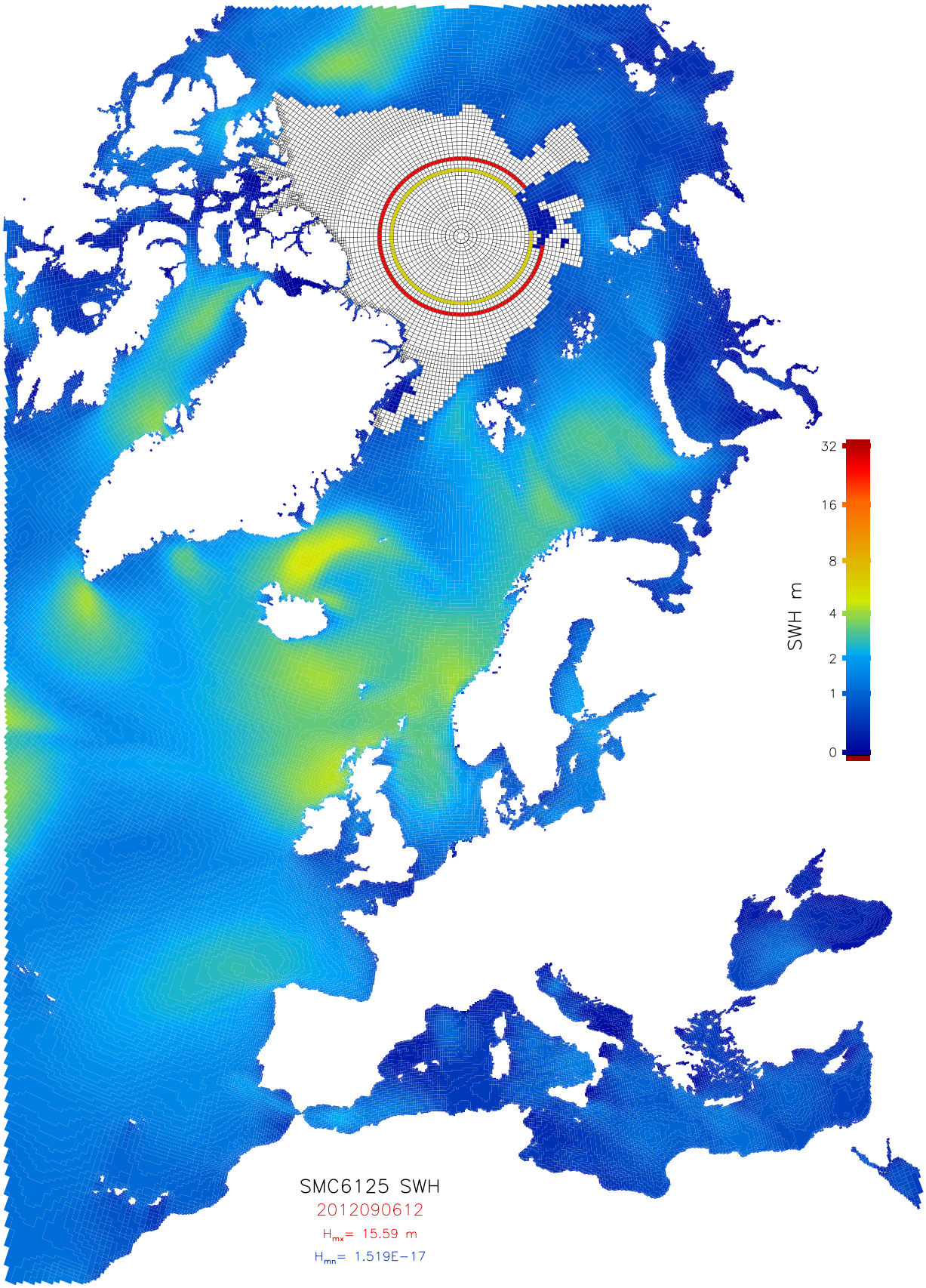

Fig. 2 SWH from SMC6125 model at 1200 hr on 06 September 2012, close to the minimum Arctic sea ice in summer 2012

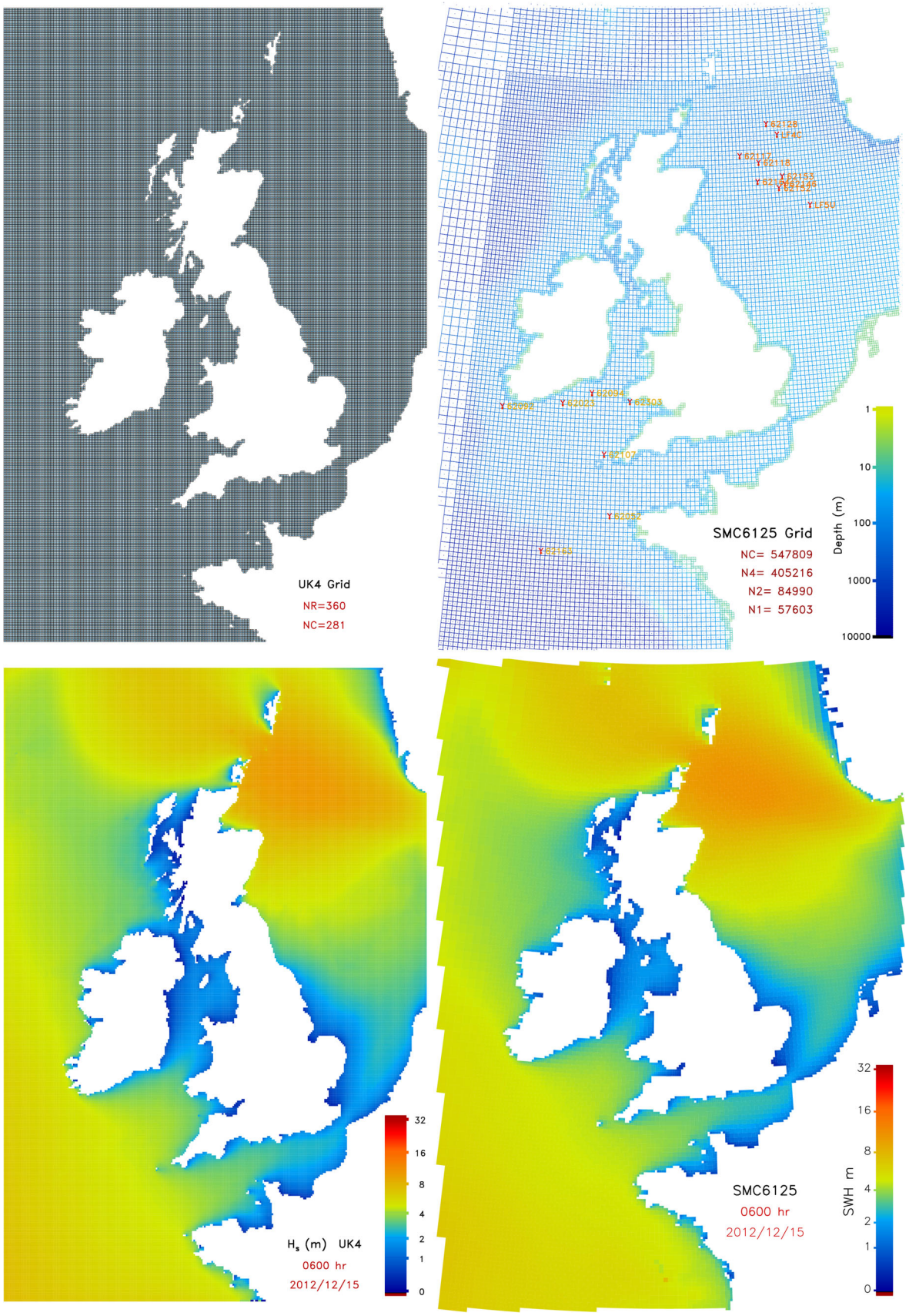

Fig. 3 Comparison of UK4 and SMC6125 grids and SWH on 15 December 2012

Arctic part of the SMC6125 model (above the yellow circle in Fig. 1 or Fig. 2) has not been activated for this study. The SWH plot also confirms that the energy flux across transition between different resolution parts, such as crossing the merging parallels at high latitudes and from the coarse base-level 25-km resolution to refined 12-km European region, is smooth and continuous. This smooth transition between different resolution parts is a direct benefit to this multi-resolution grid. Nested grids use more complicated two-way nesting techniques to achieve the same effect (Tolman 2008).

3.2 Comparison of the SMC6125 model with operational models

As the unified SMC6125 model is intended as an alternative to a traditional operational global and regional wave model suite, it is then compared with the Met Office present operational suite, comprising a global 35-km multi-grid model (G35), the European 8-km model (EU8) and the 4-km model around the UK waters (UK4). The G35 model uses a multi-grid version of the WAVEWATCH III model with the middle main domain covering from 65.5° S to 72.0° N at a resolution of about 35 km and two polar stripes connecting the main domain to the polar regions at reduced resolution of about 60 km.

The EU8 model is framed on a rotated grid, covering roughly 25° W to 45° E and 30° N to 70° N at constant resolution of 0.08° at both directions. The rotated N-Pole is at 177.5° E and 37.55° N, so the rotated Equator is about 52° N at the zero meridian, or approximately crossing London, UK. Because the SMC6125 grid uses standard latitude-longitude meshes, its size-2 longitudinal resolution in the refined European region has shrunk close to that of the EU8 model due to increased latitudes.

The UK4 model is also on the same rotated grid as the EU8 model but at the higher resolution of 0.04° for both latitude and longitude dimensions. Its grid and SWH plots are shown in Fig. 3 alongside the corresponding one from the SMC6125 model. The size-1 cell is very close to the UK4 cell while the size-2 cells are more than doubled the UK4 cells. So, the SMC6125 grid is coarser than the UK4 except for near the coastlines. Nevertheless, the SWH on 15 December 2012 from both models are very close as shown in the lower two panels in Fig. 3.

A comparison of model run times for the different modelling systems on the IBM Power 7 supercomputer used at the Met Office indicates that the G35 model required 0.36 node hours (32 processors to a node) per 24-h period predicted. The EU8 required 0.1 node hours and the UK4 model 0.09 node hours. The SMC6125 model required 0.49 node hours. Thus, the overall cost of running the SMC6125 model in these experiments was approximately the same as that needed for either the G35-EU8 or G35-UK4 nested set-ups. This is despite the SMC6125 model being approximately 30 % better resolved in the open ocean, having similar resolution to the EU8 in European seas and using an order of magnitude higher resolution than the G35 around all other global coastlines.

3.3 Choice of source terms

There are various choices for the source terms in WAVEWATCH III, and the Met Office operational wave model selection is a compromise between accuracy and efficiency. When not constrained by assimilating observations, wave model accuracy is primarily affected by the wind field used to force the model, the source term package applied in the wave model and then the grid scheme. To isolate the effects of the SMC grid, the SMC6125 configuration was compared with runs of the Met Office operational global-nested regional model set-up using the same forcing and physics package for all model runs. Wind forcing at 10 m above the sea surface was taken from the operational analysis cycle of the Met Office global atmospheric model at a resolution of approximately 25 km. The source term package is based on WAM-cycle4 (WAMDI group 1988) and uses similar parameter settings to those described by Bidlot (2012), but with the addition of a limited swell dissipation based on the scheme available in WAVEWATCH III (ST3 option) following Ardhuin et al. (2010). This approach was adopted to reduce wave height over-prediction bias in the tropics which occurred in the global wave model when using the WAM-cycle4 source terms only.

Table 1 Source term parameter settings used in WAVEWATCH III for this study

Name list	Parameter	Value
SIN3	BETAMAX	1.28
	ZALP	0.008
	ALPHA0	0.006
	SWELLFPAR	3
	SWELLF	0.2
	SWELLF2	−0.012
	SWELLF3	−0.009
	SWELLF5	0.4
	Z0RAT	0.04
SDS3	SDSC1	−1.33
	SDSDELTA1	0.5
	SDSDELTA2	0.5
SBT1	GAMMA	−0.038
SDB1	BJALFA	0.01
FLX3	CDMAX	3.5E-3
	CTYPE	0

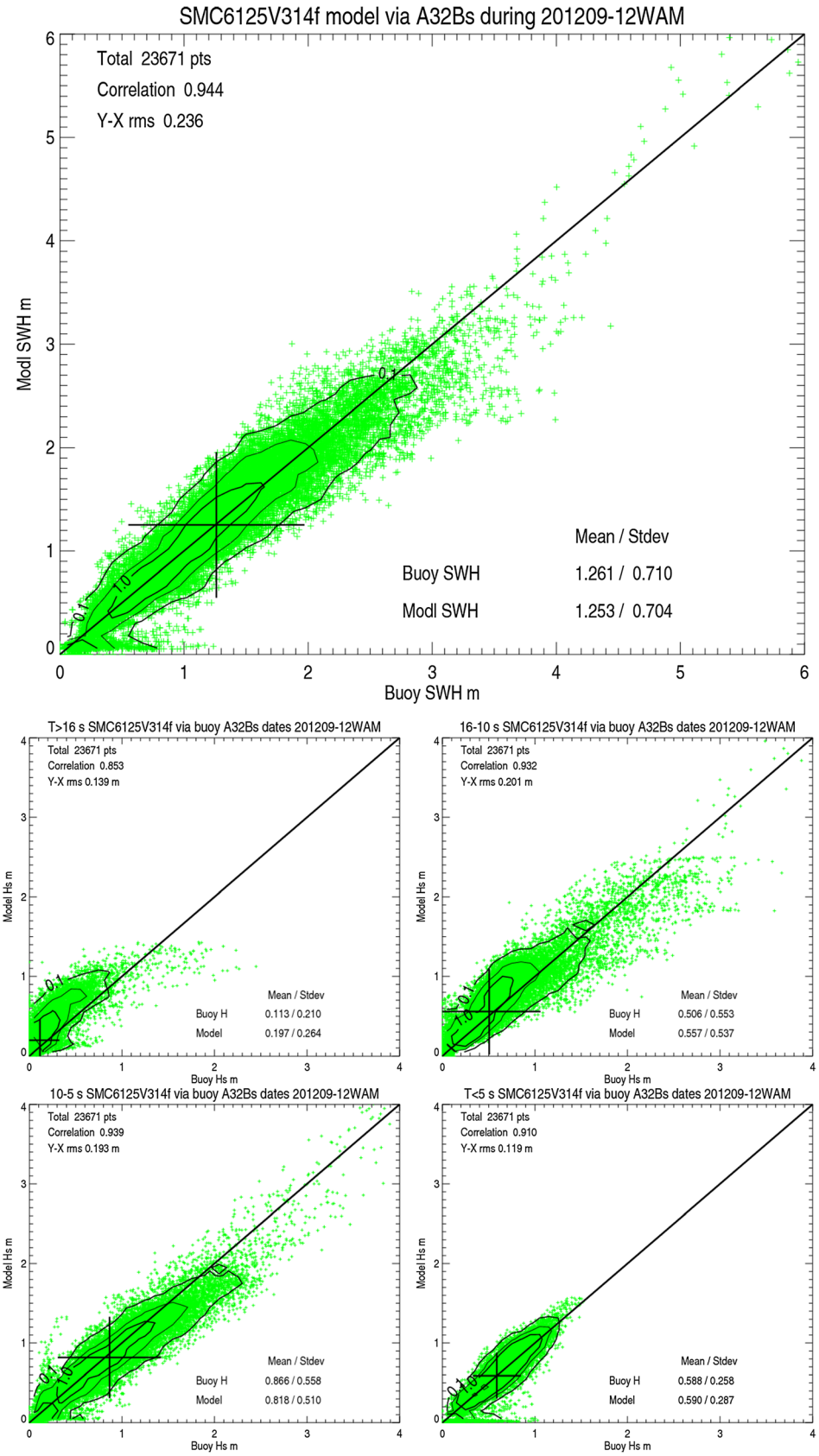

Fig. 4 Comparison of SMC6125 model SWH with 30 spectral buoys form 1 September to 31 December 2012 (*top single panel*) and their four-bin SRWH break down (*bottom four panels*)

Tuning of the ST3 source term has been done with the help of the four-bin sub-range wave height (SRWH), which is similar to the commonly used SWH but integrated over a limited sub-range of the wave spectrum (Li and Holt 2009). The four-bin SRWH reveals performance of the wave model in different spectral ranges and roughly indicates the ability of the model to represent wind sea and swell. The SRWH can be measured against wave spectral observations, such as wave spectral data from buoys. So, source term parameters controlling the wave energy input can be tuned with the SRWH in the wind sea range, and wave energy dissipation parameters can be adjusted with the swell SRWH components. The final parameter settings for the ST3 source term used in this study are given in Table 1.

4 Validation results and discussions

4.1 Validation of the SMC6125 model with buoys

To demonstrate overall performance of the model and source term choice, the SMC6125 model is first validated with wave spectra from 32 NDBC buoys over 4 months, September–December 2012 (available online at http://www.ndbc.noaa.gov). See Fig. 4 in Li (2012) for the spectral buoy locations marked with 'Y' symbols. These spectral buoys are mainly scattered along the coastlines of USA, and they represent typical wave regimes: enclosed waters of wind sea only, like the Gulf of Mexico; open oceans with mixed wind sea and swells, such as the Pacific Ocean around the Hawaii Islands, and coastal regions for most of the buoys. These buoys yield 1-D ocean surface wave spectra at roughly 0.01-Hz interval from 0.02 to 0.5 Hz at each hour. The model 2-D spectra at the closest grid points and the model time steps are compared with the buoy data.

Figure 4 shows scatter plots for both the SWH and four-bin SRWH. It is evident that both the total SWH and the four-bin SRWH are in good agreement with the buoy observations. The rms error of the model against 23,671 entries of buoy SWH data is about 0.24 m as shown in the top panel of Fig. 4. The correlation is as high as 0.94. The mean SWH bias is less than 0.01 m. The model performance is balanced over the whole spectral range as the four-bin SRWH indicates. The first two bins (wave period T>16 s and T between 10 and 16 s) may be considered to represent the swell and the last two bins (T between 5 and 10 s and T<5 s) are characteristic of the wind sea. The four scatter plots in Fig. 4 (lower four panels) show similarly small rms errors and high corrections for all the four-bin SRWH components. The bias varies from −0.05 to 0.08 m for the four bins with the best match (0.02 m) in the pure wind sea bin (T<5 s). This indicates a very good tuning of the wind input source term to the forcing wind. The increased bias (0.08 m) in the swell bin (T>16 s) means that swell field is slightly higher in the model than the buoy spectra, which could be caused for many possible reasons. For instance, it could be partially due to the dissipation not being strong enough or it might be missing some coastal blocking. It could also be the result of the coastline approximations as steps or truncation errors in the propagation schemes. Nevertheless, the overall rms errors are small and the results are satisfactory.

4.2 Regional shelf sea comparisons of the SMC6125 model with operational models

To assess the performance of the SMC6125 in waters covered by the Met Office regional models, a detailed comparison has been made in a number of sea areas around the UK continental shelf. The verifying data in these cases were taken from in situ platforms contributing to the JCOMM inter-comparison of operational ocean wave forecasting systems (Bidlot et al. 2007). Table 2 presents a summary of bias and root mean squared error (RMSE) statistics from these areas and indicates that overall levels of performance from the SMC6125 and the two regional nested models are extremely close. In a number

Table 2 SWH verification statistics for UK sea areas

Area	SMC6125		G35		EU8		UK4	
	Bias	RMSE	Bias	RMSE	Bias	RMSE	Bias	RMSE
UK	0.07	0.37	0.09	0.40	0.03	0.37	0.05	0.37
Southwest Approaches	0.01	0.38	0.10	0.45	0.01	0.38	0.04	0.38
Northwest Approaches	−0.04	0.45	−0.02	0.47	−0.10	0.46	−0.08	0.45
Northern North Sea	0.14	0.40	0.11	0.40	0.11	0.39	0.16	0.40
Central North Sea	0.09	0.35	0.12	0.37	0.06	0.35	0.07	0.35
Southern North Sea	0.09	0.25	0.05	0.27	0.04	0.24	0.05	0.24
Irish Sea	−0.09	0.25	−0.11	0.28	−0.10	0.25	−0.12	0.25

Statistic values are given in metres

of cases, the G35 scores fall close to those of other models, indicating that the primary contributions to errors will result from wind forcing and the model source terms.

Nevertheless, the grid choice can be seen to have an effect on the model skill. More detailed inspection of the verification illustrates the performance of the SMC6125 model in environments where the proximity of land will affect the fetch to the measurement locations in a number of directional sectors. The 'Y' symbols in the top-right panel of Fig. 3 indicate two groups of buoys and platforms used for the comparison, one group in the southwest approach of England (marked with yellow IDs) and the other in the central North Sea area (with orange IDs).

Figures 5 and 6 show results of a verification comparison between the SMC6125 and the G35, EU8 and UK4 wave models. In the Southwest Approaches case (Fig. 5), the

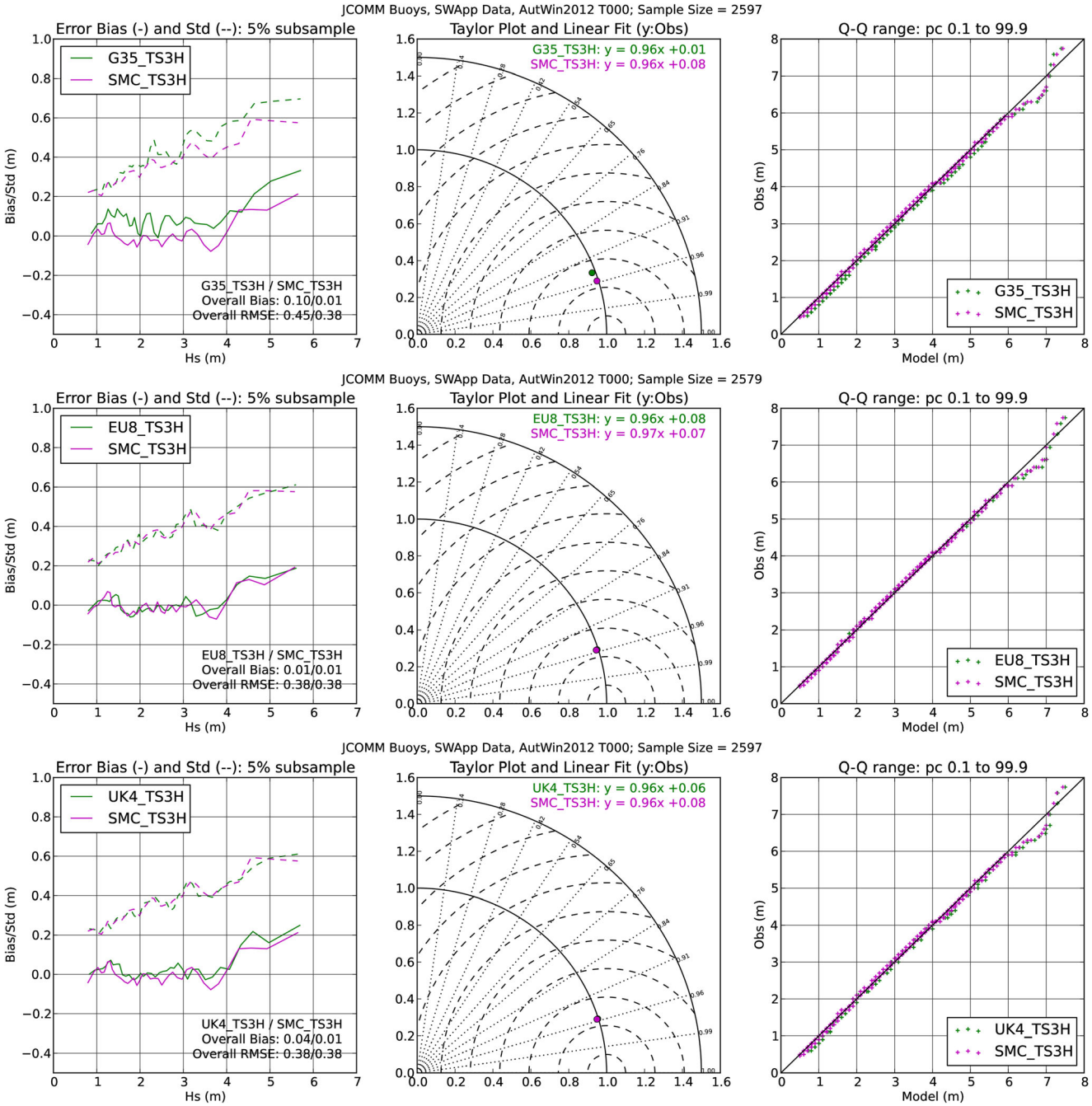

Fig. 5 Comparison of performance of the Met Office operational Global 35-km, European 8-km and UK 4-km wave models with the SMC6125 model in prediction of significant wave height for in situ platforms in the Southwest Approaches to the UK. *Plots* in columns from *left* to *right* show bias and RMSE through 5% subsamples of the model significant wave height range; Taylor plot and quantile-quantile plot of data at 0.1% intervals from 0.1–99.9%

influence of waves generated in open waters of the Atlantic is important for waves from prevailing westerly sectors. The verification for this area tests the boundary condition properties of the nested models and effect of cell refinement in the SMC6125 model, in addition to providing a check on how the models handle sheltering and fetch limitation effects associated with the peninsulas of southern Ireland, western England and northwest France. In the case of the Central North Sea (Fig. 6), a long fetch is only established for waves from the north and this verification should highlight how each model deals with fetch representation in the region.

Each figure comprises (by column) a comparison of bias and error standard deviation based on 5 % subsamples of the modelled SWH, a Taylor plot and a (0.1 % stepped) quantile-quantile plot of model versus observation and (by row) the comparison between the SMC6125 model and the G35 and nested EU8 and UK4 configurations. In Figs. 5 and 6, and indeed for other regional cases, the quantile-quantile

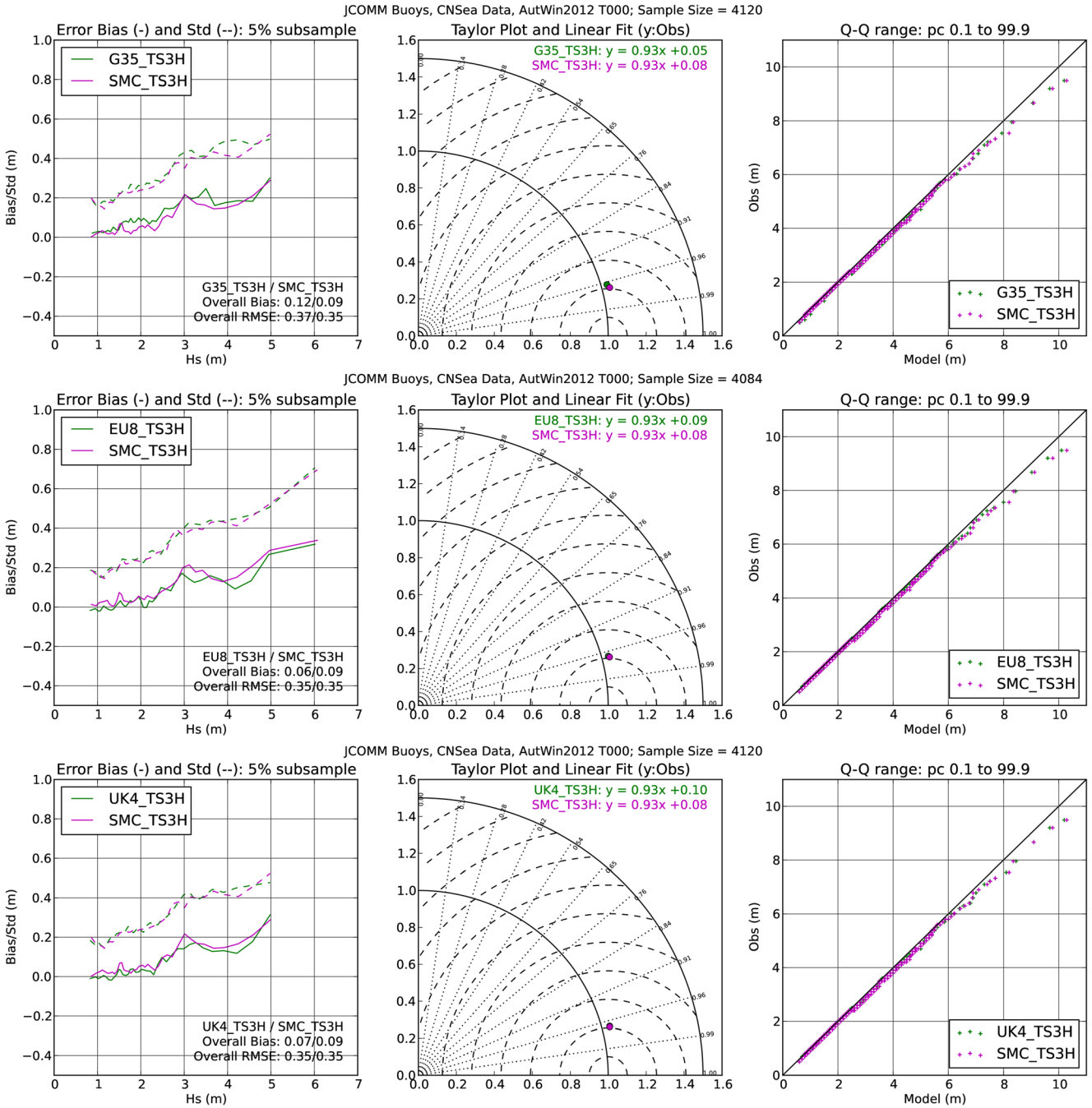

Fig. 6 Same as Fig. 5 but for in situ platforms in the Central North Sea

comparisons show good agreement between the modelled and observed wave height climate up to around the 98th percentile, so in general, the model configurations can be thought of as replicating the background climate well.

The upper row of panels in Fig. 5 compares the G35 and SMC6125. A substantive improvement in bias, error standard deviation and correlation (shown by a shift toward the *x*-axis in the Taylor plot) can be seen for the SMC6125 data. The central and lower row of panels, which compare the SMC6125 respectively to the EU8 and UK4 configurations suggest a negligible difference between the models. In the Central North Sea case (Fig. 6), the differences between all models are more limited, although a small improvement occurs in error standard deviation between the G35 and other configurations, and a more substantive improvement is seen in bias. Speculating somewhat, it is likely that the more marked improvement between G35 and higher resolution configurations in the Southwest Approaches is most heavily influenced by the better representation of headland sheltering that the resolution increase enables.

Overall, these examples suggest that the SMC model is capable of meeting its designated aims, i.e. to provide an improvement beyond a regular grid global model and achieve similar levels of accuracy to a high resolution nested model in regional seas. Although subject to further testing, these results appear to be robust to changes in the source term physics used by the model. In the test scenario presented in this paper, where wind data and source term schemes were identical for each configuration, the SMC model has been demonstrated to have almost identical performance to a similarly resolved and a higher resolution regional model. Within an operational forecasting framework, however, the regional systems may be associated with high resolution wind data and be subject to particular source term refinements relevant to the local model but inappropriate for a global system. For a single global model to compete with this type of system, further work may be necessary to introduce 'blended' wind (and ocean) forcing to the wave model and to obtain a source term parameterisation that is truly independent of the need to tune between models with different grid scalings.

5 Conclusions

The SMC grid has been implemented in WAVEWATCH III and tested as an alternative to an operational global-nested model suite. In a controlled test, where wind forcing and physics schemes are the same for all models, results indicate that the SMC6125 is better than the G35 global model and comparable with two regional models at higher resolutions. The improvement against the global model is likely to directly result from improved representation of coastline sheltering and fetch length. The results suggest that, if regional high resolution wind forcing could be blended with the global wind field and used to drive the high resolution part of the SMC6125 model, the unified wave model is capable of replacing a global and nested regional operational suite. The advantages of this approach would be to improve computational efficiency and simplify configuration management without a sacrifice of accuracy.

Acknowledgments The authors are grateful to the two anonymous reviewers and the editor, Dr Oyvind Breivik, for their useful suggestions to improve the manuscript.

References

Ardhuin F, Rogers E, Babanin A, Filipot JF, Magne R, Roland A, van der Westhuysen A, Queffeulou P, Lefevre JM, Aouf L, Collard F (2010) Semiempirical dissipation source functions for ocean waves. Part I: definition, calibration and validation. J Phys Oceanogr 40: 1917–1941

Bidlot JR (2012) Present status of wave forecasting at ECMWF. Proc ECMWF Workshop on Ocean Waves, ECMWF, Reading, UK, pp 1–15

Bidlot JR, Li JG,JR Wittmann P, Fauchon M, Chen H, Lefevre JM, Bruns T, Greenslade D, Ardhuin F, Kohno N, Park S, Gomez M (2007) Inter-comparison of operational wave forecasting systems. Proc 10th International Workshop on Wave Hindcasting and Forecasting, Hawaii, USA, 21 pp

Booij N, Holthuijsen LH (1987) Propagation of ocean waves in discrete spectral wave models. J Comput Phys 68:307–326

Chawla A, Tolman HL (2008) Obstruction grids for spectral wave models. Ocean Model 22:12–25

Hardy TA, Mason LB, McConochie JD (2000) A wave model for the Great Barrier Reef. Ocean Eng 28:45–70

Li JG (2008) Upstream non-oscillatory advection schemes. Mon Wea Rev 136:4709–4729

Li JG (2011) Global transport on a spherical multiple-cell grid. Mon Wea Rev 139:1536–1555

Li JG (2012) Propagation of ocean surface waves on a spherical multiple-cell grid. J Comput Phys 231:8262–8277

Li JG, Holt M (2009) Comparison of ENVISAT ASAR ocean wave spectra with buoys and altimeter data via a wave model. J Atmos Ocean Technol 26:593–614

Li JG, Saulter A (2012) Assessment of the updated Envisat ASAR ocean surface wave spectra with buoy and altimeter data. Remote Sens Environ 126:72–83

Popinet S, Gorman RM, Rickard GJ, Tolman HL (2010) A quadtree-adaptive spectral wave model. Ocean Model 34:36–49

Rasch PJ (1994) Conservative shape-preserving two-dimensional transport on a spherical reduced grid. Mon Wea Rev 122:1337–1350

Roland A, Cucco A, Ferrarin C, Hsu TW, Liau JM, Ou SH, Umgiesser G, Zanke U (2009) On the development and verification of a 2-D coupled wave-current model on unstructured meshes. J Marine Sys 78 SUPP: S244-S254

Tolman HL (1991) A third-generation model for wind waves on slowly varying unsteady and inhomogeneous depths and currents. J Phys Oceanogr 21:782–792

Tolman HL (2002) Alleviating the garden sprinkler effect in wind wave models. Ocean Model 4:269–289

Tolman HL (2003) Treatment of unresolved islands and ice in wind wave models. Ocean Model 5:219–231

Tolman HL (2008) A mosaic approach to wind wave modeling. Ocean Model 25:35–47

Tolman HL, Balasubramaniyan B, Burroughs LD, Chalikov DV, Chao YY, Chen HS, Gerald VM (2002) Development and implementation of wind-generated ocean surface wave models at NCEP. Weather Forecast 17:311–333

Tolman HL, Banner ML, Kaihatu JM (2013) The NOPP Operational Wave Model Improvement Project. Ocean Model 70:2–10

Tolman HL and the WAVEWATCH III® development group (2014) User manual and system documentation of WAVEWATCH III® V4.18. Tech. Note 316, NOAA/NCEP/MMAB, 311 pp

WAMDI group (1988) The WAM model—a third generation ocean wave prediction model. J Phys Oceanogr 18:1775–1810

WISE group (2007) Wave modelling—the state of the art. Progress Oceanogr 75:603–674